ICAS 84-3.4.3

COMPARISON OF THE MEASURED AND COMPUTED LOAD-DEFLECTION-BEHAVIOUR OF SHEAR-LOADED FIBER REINFORCED PLATES IN THE POSTBUCKLING RANGE

H. Tunker
Institut für Flugzeugbau und Leichtbau
Technical University of Braunschweig
Braunschweig FRG

Abstract

In this paper the particular effects are presented, which affect the behaviour of fibre reinforced plastics in the postbuckling range. Results are shown for shear-loaded quadratic plates.
Theoretical calculations are carried out by a mixed finite element method, based on geometrically nonlinear theory. The calculation of the stiffness properties is layer-oriented.
The real behaviour of plates is investigated in parallel carried out experiments. The plates are tested in a shear frame which makes possible a good comparison between theoretical and experimental results.
The matrix failure criterion and the following loss of stiffness are considered in the theoretical calculations, with that the results are comparable even above the matrix failure boundary.

I. Introduction

If you examine the increase of direct operating costs (DOC) of air liners it becomes necessary to spend more research and development in the lightweight construction of air liners and small planes, Figure 1. It is very important that beside the general advance in price the increase of the parts of amortization and especially fuel is dominant.

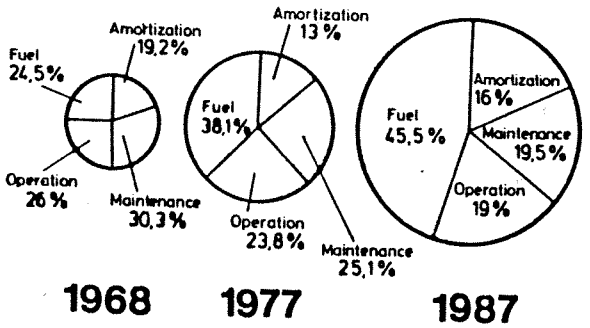

Figure 1. Expansion of DOC

The possibilities for reduction of consumed fuel mass can be shown - in a simply representation - by the formula of Breguet for the range of an air liner, Figure 2. That are the specific fuel consumption, the aerodynamical quality and the structural quality. The last will be regarded in this paper

Formula for the range of Breguet

$$\frac{m_F}{m_{TOW}} = 1 - e^{\frac{-R \cdot b_S \cdot g}{v \cdot E}}$$

$$m_F = m_{TOW}\left(1 - e^{\frac{-R \cdot b_S \cdot g}{v \cdot E}}\right)$$

$$= (m_{OE} + m_{UL} + m_F)\left(1 - e^{\frac{-R \cdot b_S \cdot g}{v \cdot E}}\right)$$

* Specific fuel consumption
* Aerodynamic quality
* Structural quality

Figure 2. Effects on fuel consumption

Today one of the remarkable tasks in aircraft construction is the improvement of structural quality. That contains the application of new materials, such as fiber reinforced plastics (FRP), and the use of better computation-, simulation- and proof-procedures, for example Finite--Element-Method (FEM) or conditioned fatigue test, Figure 3

Structural quality — Light construction

Materials

— *Plywood*

— *Aluminium-alloys*

— *Fiber-reinforced plastics (FRP)*

Calcution methods | Testing procedures

— *Beams*

— *Thin-walled construction*

— *Finite Elements (FEM)*

— *Buckling loads*

— *Postbuckling Behaviour*

— *Time strength*

— *Fatique Behaviour*

— *Fracture mechanics*

Figure 3. Structural Quality

In this paper the behaviour of shear-loaded glass-fiber-reinforced plates with selected boundary conditions and imperfections is investigated. We choose the conditions in the way, so that they can be simulated intests and so that they are similar to usually constructions, Figure 4. By variation of the parameters a wide range of material and geometry combinations could be investigated.

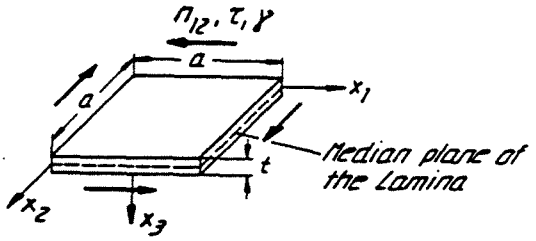

○ *Materials*

GFRP $\gamma_{Vol} = 50\,\%$

Fiber angle $= \pm 45°, 0°|90°$

(*Al Cu Mg 2*)

○ *Boundary conditions*

all sides clamped

○ *Imperfection*

Figure : (1-cos) -*like*

Amplitude : 1÷50% *of plate thickness*

Figure 4. Definition of the investigated system

The attempt was made, to synthesize the results in the theoretical investigations only from fiber and matrix properties but nevertheless to get comparable results by the theoretical and experimental investigations.

II. Theoretical Investigation

Starting point for the theoretical investigations are the properties of the matrix and the fiber. The material law of a unidirectional (UD) lamina is composed from these properties by special assumptions for fiber arrangement and existence of defects (1), Figure 5. The material law of the lamina is found by integration of the material laws of the UD-Laminas.

Assumptions:

Matrix — *Isotropic resim*

Fiber — *Transversal-isotropic fiber*

Quadratic packing of circular fibers

Perfect arrangement

$$E_{\parallel} = E_{F\parallel} \cdot \phi_F + E_M \cdot (1 - \phi_F)$$

$$E_{\perp} = E_M \cdot \left\{ 1 - 2\sqrt{\frac{\phi_F}{\pi}} - \frac{\pi}{2 \cdot \left(1 - \frac{E_M}{E_{F\perp}}\right)} + \right.$$

$$\left. + \frac{}{\left(1 - \frac{E_M}{E_{F\perp}}\right)\sqrt{1 - 4\frac{\phi_F}{\pi}\left(1 - \frac{E_M}{E_{F\perp}}\right)^2}} \arctan \sqrt{\frac{1 + 2\sqrt{\frac{\phi_F}{\pi}}\left(1 - \frac{E_M}{E_{F\perp}}\right)}{1 - 2\sqrt{\frac{\phi_F}{\pi}} \cdot \left(1 - \frac{E_M}{E_{F\perp}}\right)}} \right\}$$

Figure 5. Material laws of UD-Laminates, composed out of fiber and matrix data

First the critical buckling stress shall be regarded, comparing the results for FRP and the common aluminium alloys, Figure 6.

Only examining the critical buckling stresses, the application of FRP doesn't seem to be iustified. But integrating the weight of the plates, what means looking at the weight-related buckling stresses, shows possible advantages of FRP - especially carbon FRP, Figure 7

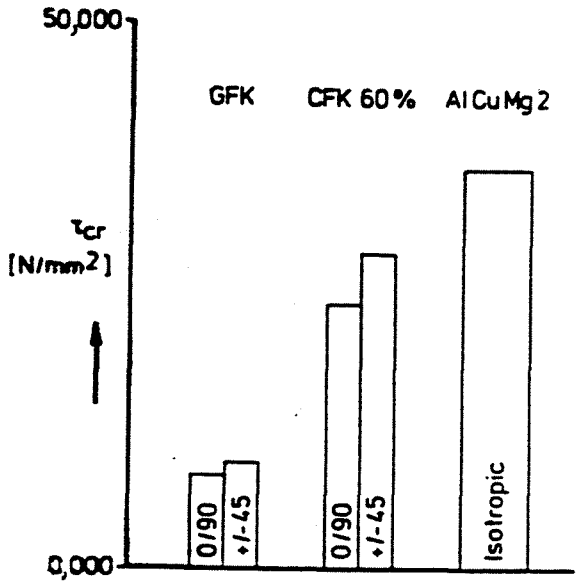

Figure 6. Buckling stresses

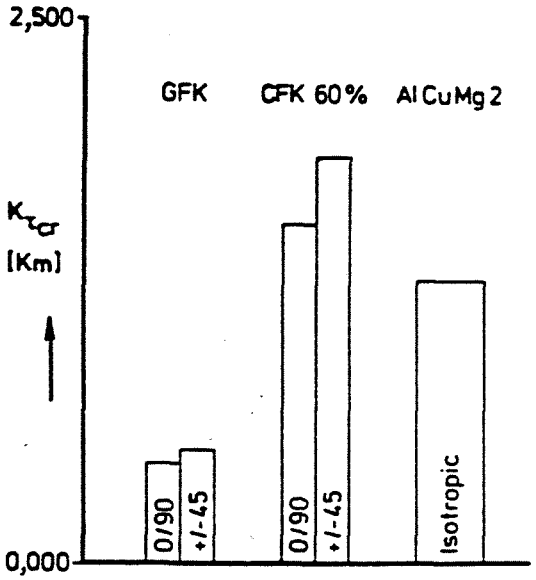

Figure 7. Weight-related buckling stresses

The failure of FRP is in this paper described by the intralaminar matrix failure (Matrix failure) and fiber failure criteria, based on the works of PUCK (2), Figure 8

Then the failure bounds and an effort can be defined. Effort means the relation between applicated load and failure bound, Figure 9. With this effort a conversion of loads and efforts will be possible.

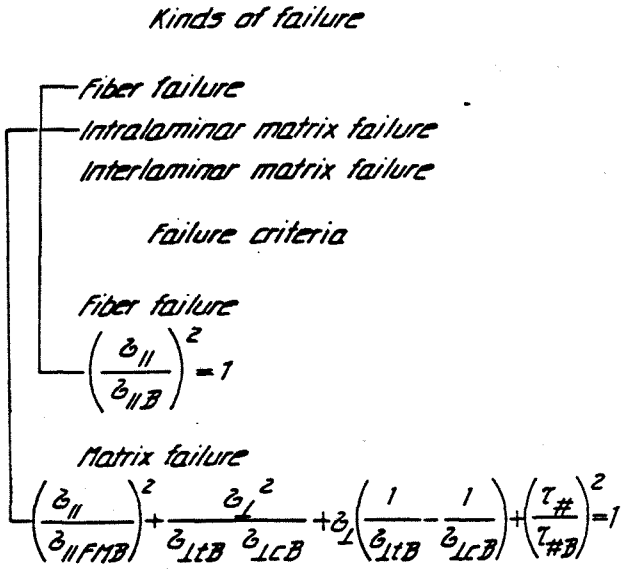

Figure 8. Failure of reinforced plastics

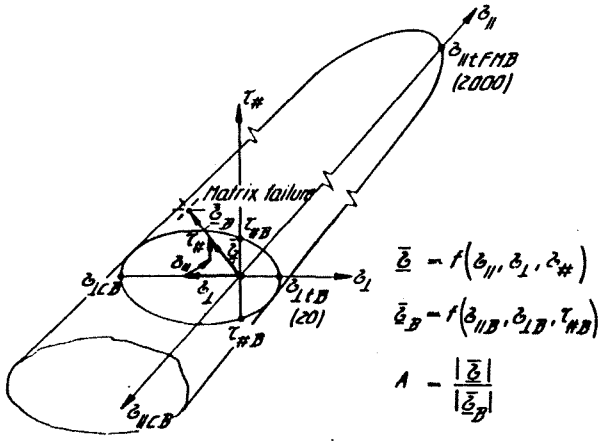

Figure 9. Effort at matrix failure

The postbuckling behaviour is investigated by an FEM-system, using a mixed linear formulation. Only linear distributions are selected, but for deformations and the important cutting forces. Additional, even the stiffness of the plate can be linear distributed, Figure 10

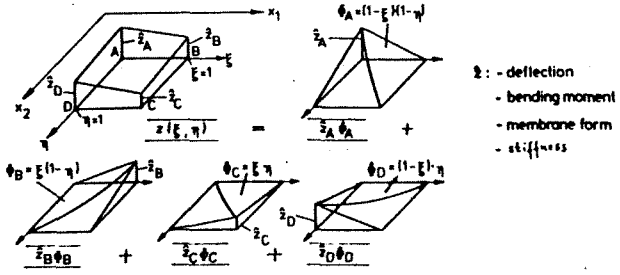

Figure 10. Mixed finite element with linear distributed variables for geometrically nonlinear problems

A look at the load-deformation-behaviour of the central point of the plate shows, that the behaviour of isotropic material is just between the behaviour of FRP with $0^0/90^0$ and $\pm 45^0$ fiber orientation, generated by the different relations of the parts of the material laws, Figure 11.

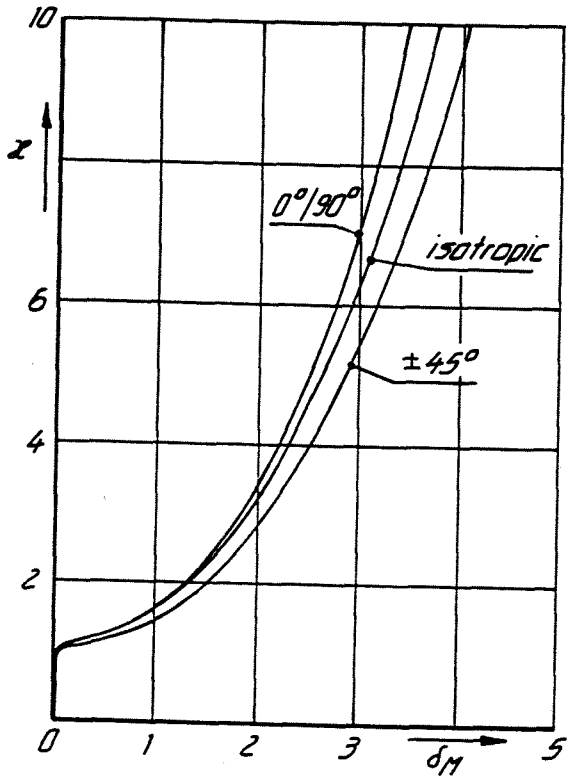

Figure 11. Load factor $\alpha = \tau_m / \tau_{cr}$ vs relative deflection $\zeta_M = w_M / t$

Figure 12 shows the deformation of the plate above the buckling load, a great buckle in the middle region and two inverse buckles in the diagonal direction. This is called a "symmetric" mode. Increase of the load will lead to more discrete buckles, retaining the symmetrical mode.

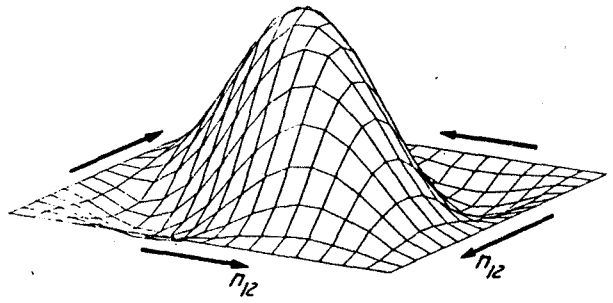

Figure 12. Deformation above critical buckling load

The loss of shear stiffness of a shear loaded structure above the buckling load is distinctly visible in the strong increase of the shear angle by increasing loads, Figure 13. In this kind of consideration, "more orthotropic" materials like CFRP are very sensitive.

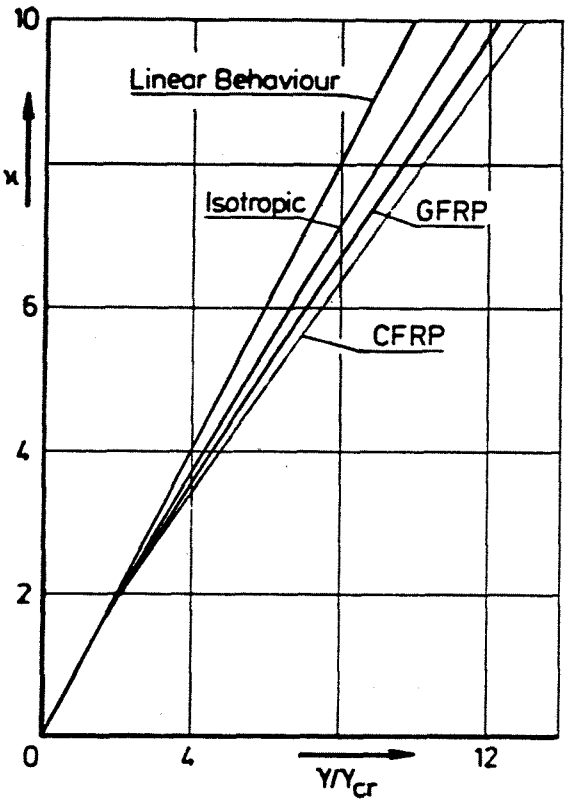

Figure 13. Load factor $\alpha = \tau_m / \tau_{cr}$ vs relative shear angle γ / γ_{cr} (fiber angle $\pm 45^0$)

Integrating the failure criteria in one diagram, Figure 14, a construction diagram can be plotted, which allows the designer to extract the buckling load, the occurence of matrix failure or fiber failure (without regard of matrix failure) for selected geometric relations and for similar materials

III. Experiments

First experiments were executed in a simple shear frame, Figure 15, to get experience with the testing technique

Then a better shear frame was developed. This frame allows direct measuring of diagonal deformation, bending deformation along the compression diagonal line and applied load, Figure 16. For the improvement of the frame behaviour the point of rotation of the supporting beams is now just in the corner of the free buckling area, without penetrating the plate.

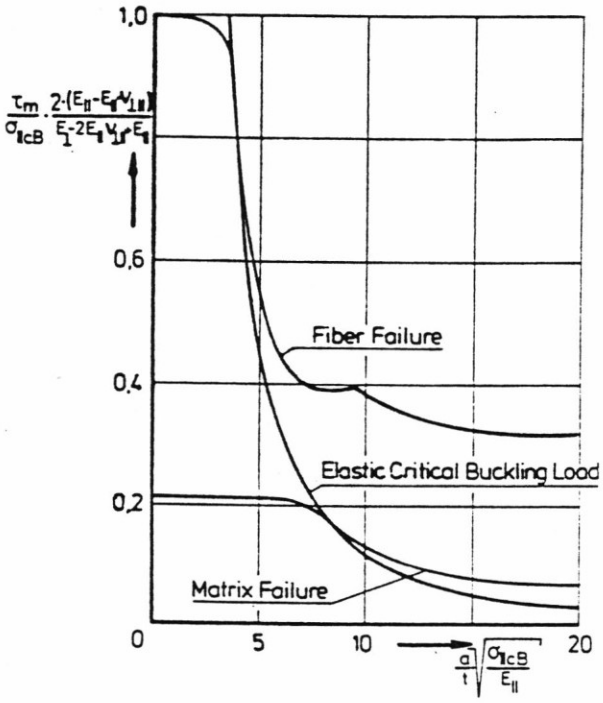

Figure 14. Elastic "limit " loads (fiber angle ± 45°)

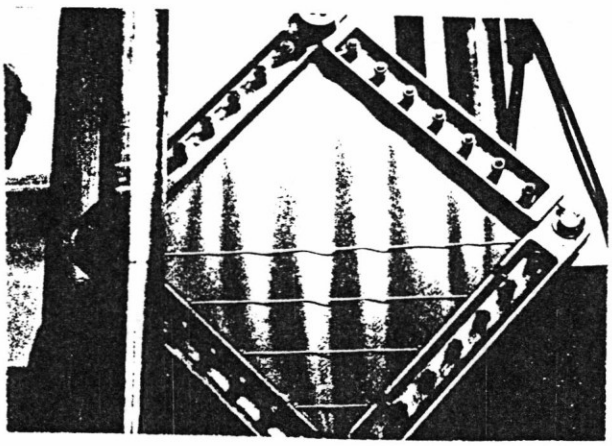

Figure 15. Simple shear frame with plate in the high postbuckling range

Figure 17 shows the disassembled frame with one testing plate beside.

The plates were cutted out of pressed plates with ± 45° or 0°/90° fiber orientation, Figure 18. Simultaneously, test specimens were extracted, to examine the material properties in ± 45° and 0°/90° direction.

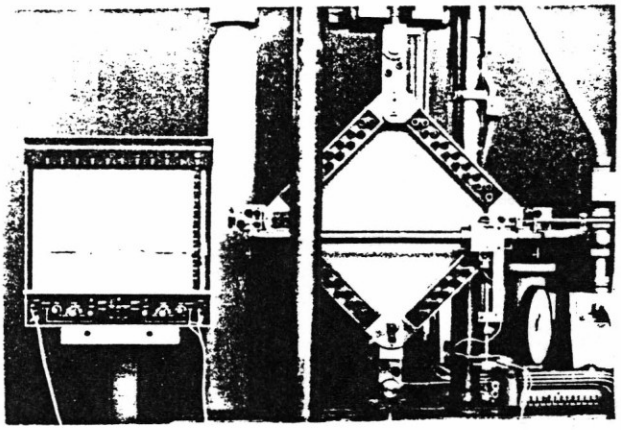

Figure 16. Test setup with plotter

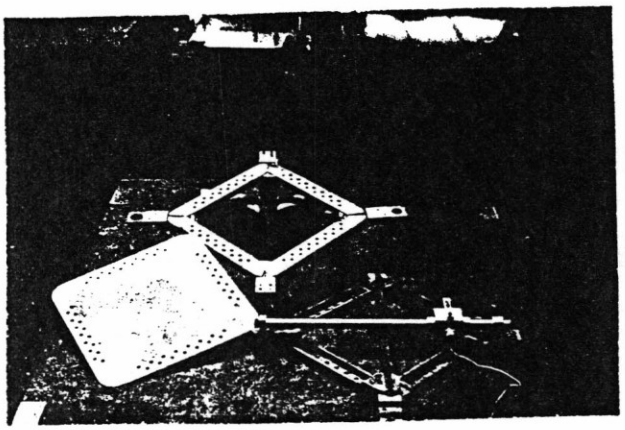

Figure 17. Disassembled frame

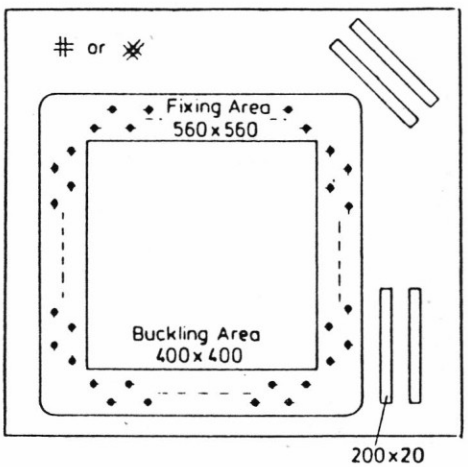

Figure 18. Cutting plan for test specimens

Results for ± 45° fiber angle. Comparing the computed and measured curves, you see that the tested plates have great imperfections (25-50 % of plate thickness). There fore the computations were done with similar imperfections, Figure 19. The simplified assumptions explain the great difference between measured and computed curves in the postbuckling range. By using a stiffness reduction scheme the influence of matrix failure could be seized, so that the curves will then again get the same tendency.

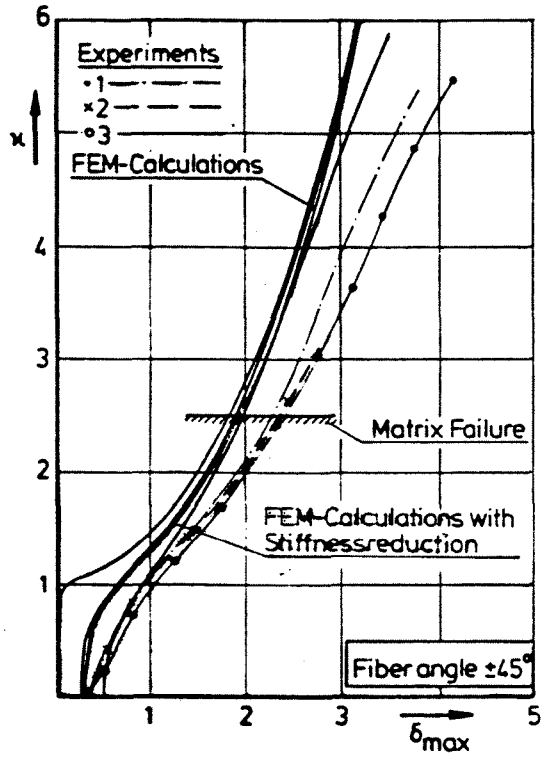

Figure 19. Comparison of computed and measured $\varkappa = \tau_m/\tau_{cr}$ vs $\delta = u_3/t$

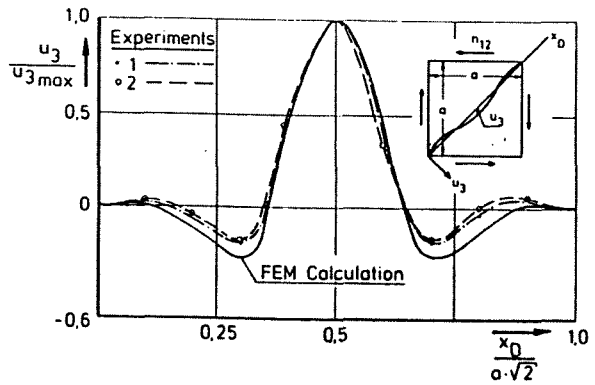

Figure 20. Bending deformation of the compression diagonal line at $\varkappa \approx 5{,}0$ (fiber angle ± 45°)

Furthermore the buckling shape could be well approximated above the critical load, Figure 20.

Also the changing in shear stiffness of the systems could be described with the stiffness reduction scheme better than with the normal scheme, Figure 21.

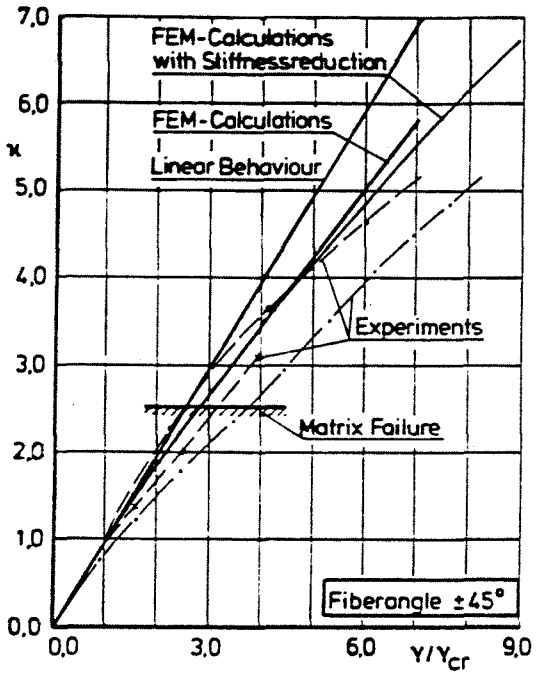

Figure 21. Comparison of computed and measured load-deflection-behaviour

Results for 0°, 90° fiber angle. By this fiber orientation you can see the effects of the dominant properties of the matrix, Figure 22, strong incresing shear angle with increasing load, unmistakable visible in the computed version with stiffness reduction.

The load-central deflection diagramm, Figure 23, shows that the moments on the support increase by the decrease of the matrix stiffness by matrix failure, which then decreases the central deflection.

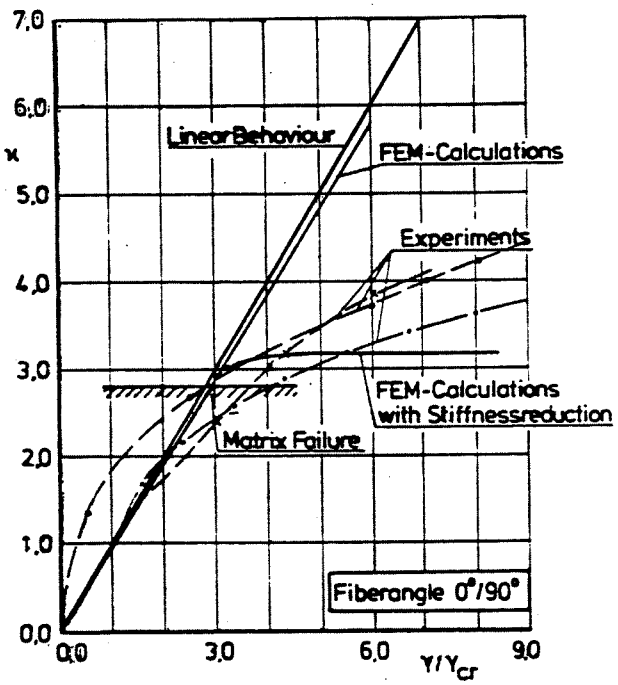

Figure 22. Comparison of computed and measured load-deflection-behaviour

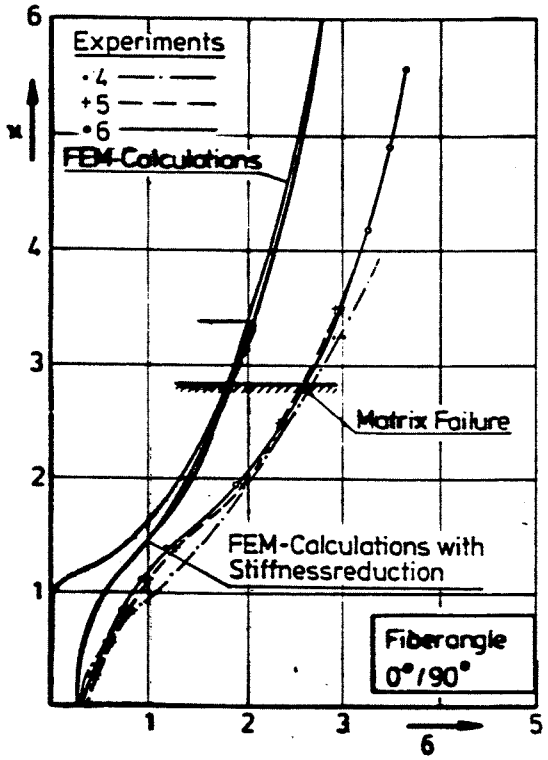

Figure 23. Comparison of computed and measured $\varkappa = \tau_m/\tau_c$, vs $\zeta = u_3/t$

IV. Conclusions

With computed and measured results of shear-loaded plates it could be shown that the application of FRP - especially CFRP - can result in weight losses in comparison to aluminium alloys and that the use can be meaningful nearly up to the matrix failure. Also the investigations showed that the influences and tendencies of the behaviour of the tested plates can be described with the given theoretical procedure. The comparability could be increased by a better fixing of the test parameters and an improvement of the computing scheme.

References

1 Handbuch Faserverbund--Leichtbau, (FVL-Handbuch) Gemeinschaftsarbeit von DFVLR, DORNIER, MBB und VFW-FOKKER

2 Puck, A. Schneider, W. On Failure Mechanisms and Failure Criteria of Filament-Wound Glass-Fibre/Resin Composites Plastics + Polymers, S.33-44 (Febr.1969)